0022-3565/99/2892-1090$03.00/0
THE JOURNAL OF PHARMACOLOGY AND EXPERIMENTAL THERAPEUTICS
Vol. 289, No. 2
Printed in U.S.A.

JPET 289:1090–1103, 1999

Two Pharmacologically Distinct Components of Nicotinic Receptor-Mediated Rubidium Efflux in Mouse Brain Require the β2 Subunit[1]

MICHAEL J. MARKS,[2] PAUL WHITEAKER,[2] JENNIFER CALCATERRA,[2] JERRY A. STITZEL,[2] AMY E. BULLOCK,[2] SHARON R. GRADY,[2] MARINA R. PICCIOTTO,[3] JEAN-PIERRE CHANGEUX,[4] and ALLAN C. COLLINS[2]

Institute for Behavioral Genetics, University of Colorado, Boulder, Colorado

Accepted for publication December 23, 1998 This paper is available online at http://www.jpet.org

ABSTRACT

Nicotinic agonist-stimulated efflux of $^{86}Rb^+$ from mouse brain synaptosomes was monitored continuously by on-line radioactivity detection. The concentration-effect curve following a 5-s stimulation with acetylcholine was biphasic (EC_{50} = 7.2 and 550 μM). α-Bungarotoxin (100 nM) did not inhibit the response, but dihydro-β-erythroidine (DHβE) blocked both phases with differing potency (average IC_{50} = .22 and 8.9 μM for responses activated by low and high acetylcholine concentrations, respectively). Differential sensitivity DHβE inhibition was used to measure stimulation of $^{86}Rb^+$ efflux by 17 nicotinic agonists, which differed markedly in potency and efficacy. All agonists were more potent at the DHβE-sensitive site. Both components were inhibited by the six antagonists tested. Methyllycaconitine and DHβE were more potent for the DHβE-sensitive component, whereas hexamethonium was more potent at the DHβE-resistant component. Both DHβE-sensitive and DHβE-resistant responses were reduced more than 95% in β2-null mutant mice, establishing the requirement for the β2 subunit for both components. Both components were widely, but not identically, distributed throughout the brain. The DHβE-sensitive component appears to be identical with agonist-stimulated $^{86}Rb^+$ efflux described previously and is likely to be mediated by α4β2 receptors. The DHβE-resistant component is a novel, active, and widely distributed response mediated by nicotinic receptor(s) that also require the β2 subunit.

Nicotine and nicotinic agonists elicit many diverse responses in vivo (Brioni et al., 1997). This physiological and behavioral diversity arises in part from differences in composition of, anatomical localization of, and physiological processes stimulated by nicotinic receptors. Nicotinic receptors are distributed on skeletal muscle, in the autonomic nervous system, on secretory tissue, and in the brain. In addition, nicotinic receptors themselves are complex pentameric assemblies of homologous subunits. Receptor subtypes composed of different homomeric or heteromeric combinations of subunits display markedly diverse physiological and pharmacological properties (Sargent, 1993). Responses secondary to the activation or inhibition of nicotinic receptors (such as neurotransmitter or hormonal release) also influence the response to nicotinic agonists (Wonnacott, 1997). Thus, the responses observed after acute or chronic exposure to nicotine or other nicotinic drugs are determined by a complex array of factors.

One approach to investigate the diversity of nicotinic responses in the brain is to use biochemical assays for receptor function. For example, nicotinic receptors have been shown to modulate the release of many neurotransmitters such as dopamine, norepinephrine, acetylcholine (ACh), and GABA (Wonnacott, 1997). Because nicotinic receptors are ligand-gated ion channels, measurement of the agonist-stimulated uptake or efflux of isotopically labeled Na^+, K^+ (or Rb), and Ca^{2+}, has been used to measure receptor function. Theoretically, ion flux assays have an inherent advantage of universal applicability to receptors located either presynaptically or

Received for publication September 24, 1998.
[1] This work was supported by research Grants DA-03194 and DA-10156 and Research Scientist Award (to A.C.C.) from the National Institute on Drug Abuse (Boulder, CO), by Collège de France, Association Française contre la Myopathie, and R.J. Reynolds Tobacco Company (Paris).
[2] Current address: Institute for Behavioral Genetics, University of Colorado, Boulder, CO 80309.
[3] Current address: Department of Psychiatry, Yale University, New Haven, CT.
[4] Current address: UA D1284 "Neurobiologie Moléculaire", Pasteur Institute, Paris, France.

ABBREVIATIONS: ACh, acetylcholine iodide; A-85380, 3-(2-(*S*)-azetidinylmethoxy)pyridine; ABT-418, (*S*)-3-methyl-5-(1-methyl-2-pyrrodinyl)isoxazole; DHβE, dihydro-β-erythroidine; DMPP, dimethylphenylpiperazinium iodide; MLA, methyllycaconitine; nAChR, nicotinic acetylcholine receptor; dTC, *d*-tubocurarine chloride; TMA, tetramethylammonium chloride; α-Bgt, [^{125}I]α-bungarotoxin; P2, crude synaptosomal pellet; OB, olfactory bulbs; OT, olfactory tubercles; Cx, cerebral cortex; Se, septum; Hp, hippocampus; St, striatum; Hab, habenula; Th, thalamus; HT, hypothalamus; IPN, interpeduncular nucleus; MB, midbrain; SC, superior colliculus; IC, inferior colliculus; HB, hindbrain; Cb, cerebellum.

postsynaptically and can be used for tissue prepared from any source. Receptor-mediated stimulation of $^{86}Rb^+$ efflux has been successfully applied to the measurement of receptor function in cell lines (Lukas, 1989), in cells transfected with defined nicotinic receptor subunits (Gopalakrishnan et al., 1996), and in synaptosomes prepared from rodent brain (Marks et al., 1993). One limitation of these measurements has been the relatively long sampling times (10 s to 5 min) used. Inasmuch as nicotinic receptors desensitize with prolonged stimulation and that some receptor subtypes desensitize very rapidly, the sampling times may be inadequate to measure rapidly desensitizing subtypes such as those containing α7 subunits (Couturier et al., 1990; Seguela et al., 1993; Alkondon and Albuquerque, 1993). The results presented in this paper describe studies of nicotinic agonist-stimulated $^{86}Rb^+$ efflux from mouse brain synaptosomes measured with an on-line continuous flow radiation monitor. This methodology reduces sampling time to 3 s. Two distinct components of nicotinic agonist-mediated efflux were revealed, one that was relatively sensitive to inhibition by dihydro-β-erythroidine (DHβE) and one that was less sensitive to inhibition. Nicotinic agonist activation and antagonist inhibition differed for the DHβE-sensitive and DHβE-resistant components. Failure of either [^{125}I]α-bungarotoxin (α-Bgt) or low concentrations of methyllycaconitine (MLA) to inhibit either component indicates that the α7 subunit was not involved. Both components were widely distributed throughout the brain and experiments with β2-null mutants demonstrated that each required the β2 subunit. The DHβE-sensitive component appears to be identical with a process described previously, whereas the DHβE-resistant component appears to be a unique, as yet undescribed, response that may have a major functional role in mouse brain.

Experimental Procedures

Materials. The following were purchased from Sigma Chemical Co. (St. Louis, MO): (−)-nicotine tartrate, (+)-nicotine-(+)-di-*p*-toluoyltartrate, ACh, carbachol iodide, (±)-epibatidine hydrochloride, cytisine, (±)-nornicotine, (±)-anabasine, tetramethylammonium chloride (TMA), *d*-tubocurarine chloride (dTC), hexamethonium chloride, decamethonium chloride, sodium chloride, potassium chloride, calcium chloride, magnesium sulfate, atropine sulfate, tetrodotoxin, diisopropylflourophosphate (DFP), bovine serum albumin, and polyethylenimine. The following were purchased from Research Biochemicals International (Natick, MA): (+)-epibatidine hydrochloride, (−)-epibatidine hydrochloride, (+)-anatoxin-a, DHβE, MLA, epiboxidine and, 3-(2-(*S*)-azetidinylmethoxy)pyridine dihydrochloride (A-85380). Sucrose and HEPES were purchased from Boehinger-Mannheim (Indianapolis, IN). Dimethylphenylpiperazinium iodide (DMPP) was purchased from Aldrich Chemical Co. (Milwaukee, WI). Cesium chloride and Budget Solve Scintillation fluid were purchased from Research Products International (Mt. Prospect, IL). (*S*)-3-methyl-5-(1-methyl-2-pyrrodinyl)isoxazole (ABT-418) was a gift from Abbott Laboratories (Abbott Park, IL). [^{3}H]Nicotine (81.5 Ci/mmol), [^{3}H]epibatidine (33.8 Ci/mmol), and carrier-free ^{86}RbCl were purchased from DuPont-NEN (Boston, MA). α-Bungarotoxin (initial specific activity 210 Ci/mmol) was purchased from Amersham, Inc. (Arlington Heights, IL).

Mice. Female C57BL/6J and β2 nicotinic acetylcholine receptor (nAChR)-null mutant mice (Picciotto et al., 1995) of either sex were bred at the Institute for Behavioral Genetics (University of Colorado, Boulder, CO). C57BL/6 mice were housed five per cage and β2 mutant mice were housed with like sex littermates (2–5 per cage). The mice were housed in a vivarium maintained at 22°C with a 12-h light/dark cycle (lights on from 7:00 AM to 7:00 PM). The mice were allowed free access to food (Harlan Teklad Rodent Diet) and water. Animals were 60- to 90-days old when used. Animal care and experimental procedures were performed in accordance with the guidelines and with the approval of the Animal Care and Utilization Committee of the University of Colorado, Boulder.

Synaptosome Preparation. Crude synaptosomes were prepared from mouse forebrain or dissected brain regions. Samples were homogenized by hand (20 strokes with a Teflon-glass tissue grinder) in 10 volumes ice-cold 0.32 M sucrose buffered to pH 7.5 with 5 mM HEPES. The homogenate was centrifuged at 500*g* for 10 min. The resulting supernatant was subsequently centrifuged at 12,000*g* for 20 min to yield the crude synaptosomal pellet (P2).

$^{86}Rb^+$ Uptake. The uptake of $^{86}Rb^+$ into the synaptosomal fractions was achieved by incubating the resuspended P2 for 30 min in uptake buffer (NaCl, 140 mM; KCl, 1.5 mM; $CaCl_2$, 2 mM; $MgSO_4$, 1 mM; HEPES hemisodium, 25 mM; glucose, 20 mM; pH, 7.5) containing 4 μCi of carrier-free ^{86}RbCl. The final incubation volume was 35 μl. Uptake was terminated by filtration of the sample onto a 6-mm diameter glass fiber filter (Type AE; Gelman, Ann Arbor, MI) under gentle vacuum (−0.2 atmospheres) followed by two washes with 0.5 ml of uptake buffer. Samples to be tested for the effects of ACh were incubated with 10 μM diisopropyl fluorophosphate during the final 10 min of uptake to inhibit acetylcholinesterase.

Sample Perfusion. After filtration and wash, the glass fiber filter containing the loaded synaptosomes was transferred to a polypropylene platform. Perfusion buffer (NaCl, 135 mM; CsCl, 5 mM; KCl, 1.5 mM; $CaCl_2$, 2 mM; $MgSO_4$, 1 mM; HEPES hemisodium, 25 mM; glucose, 20 mM; tetrodotoxin, 50 nM; atropine, 1 μM; bovine serum albumin (fraction V), 0.1%; pH, 7.5) was delivered to the filter at a rate of 2.5 ml/min using a Gilson Minipuls 3 peristaltic pump (Gilson, Middleton, WI). Atropine and tetrodotoxin were included in the buffer to prevent activation of muscarinic receptors and sodium channels, respectively. The 1 μM concentration of atropine is comparable to that used in studies of heterologously expressed receptors (Leutje and Patrick, 1991) and of nAChR in cell culture (Alkondon and Albuquerque, 1993, 1995). Preliminary experiments indicated that this concentration of atropine had no effect on nicotine-stimulated $^{86}Rb^+$ efflux. TTX (50 nM) inhibits a fraction of nicotine-stimulated $^{86}Rb^+$ efflux apparently resulting from secondary activation of Na^+ channels (Marks et al., 1995) and was included to block this secondary response. Buffer was actively removed using a second Gilson peristaltic pump set for a flow rate of 3.2 ml/min. The use of two pumps prevented the accumulation of perfusion buffer on the filter holding the sample. Sample effluent was pumped through a 200 μl volume flow-through Cherenkov cell in a β-RAM Radioactivity HPLC Detector (IN/US Systems, Inc., Tampa, FL) to achieve continuous monitoring of ^{86}Rb efflux from the sample. Stimulation of the synaptosomes was accomplished by diverting perfusion buffer flow through a 200 μl loop containing the test solution by means of a 4-way rotary Teflon injection valve (Alltech Associates, Inc., Deerfield, IL). Thus, stimulation time was 5 s. The $^{86}Rb^+$ efflux was monitored for 4 min and timing was adjusted so that any efflux resulting from stimulation was located in the middle of the sampling period. This timing permitted the definition of basal efflux rate measured before and after agonist application.

Agonist Application. The stimulation of samples by agonists was achieved by filling the 200 μl sample loop with a solution of defined concentration of the agonist being evaluated. Each sample was stimulated once.

Antagonist Effects. The effect of DHβE on $^{86}Rb^+$ efflux stimulated by ACh, nicotine, or epibatidine was evaluated at two concentrations of each agonist (30 and 1000 μM, 10 and 300 μM, and 0.3 and 10 μM, respectively).

The effects of α-Bgt on ACh-stimulated $^{86}Rb^+$ efflux were measured using 30 and 1000 μM ACh on samples that had been incubated with 100 nM α-Bgt for 60 min at 22°C before filtration. Perfusion buffer for these samples also contained 100 nM α-Bgt.

The effects of antagonists were examined for samples that had been perfused with the appropriate concentration of antagonist for 8 min before stimulation with either 10 μM nicotine or 10 μM epibatidine in the presence of 2 μM DHβE. Nicotine was used to stimulate in the absence of DHβE to provide data directly comparable to those obtained previously, whereas epibatidine was used in the presence of DHβE because of the large response obtained with this agonist. The agonist solutions contained the same concentration of antagonist that was used to perfuse the samples. Thus, antagonist was present before, during, and after agonist stimulation. The effect of DHβE on the response stimulated by 10 μM epibatidine was evaluated in samples that also contained either 2 μM DHβE or 2 μM MLA.

Agonist-Stimulated $^{86}Rb^+$ Efflux in Several Brain Regions. The following fifteen brain regions were dissected and P2 fractions prepared: olfactory bulbs (OB), olfactory tubercles (OT), cerebral cortex (Cx), septum (Se), hippocampus (Hp), striatum (St), habenula (Hab), thalamus (Th), hypothalamus (HT), interpeduncular nucleus (IPN), midbrain (MB), superior colliculus (SC), inferior colliculus (IC), hindbrain (HB), and cerebellum (Cb). The P2 fractions were loaded with $^{86}Rb^+$ and evaluated for the efflux stimulated by 10 μM nicotine and 10 μM epibatidine plus 2 μM DHβE. Nicotine was used to stimulate in the absence of DHβE to provide data directly comparable to those obtained previously, whereas epibatidine was used in the presence of DHβE because of the large response obtained with this agonist. To obtain adequate samples from the small brain areas (OT, Se, Hab, HT, IPN, SC, IC), tissue from several mice was pooled before homogenization.

Ligand Binding. Particulate fractions were prepared from P2 after lysis of the crude synaptosomes by three cycles of suspension in hypotonic buffer (NaCl, 14 mM; KCl, 0.15 mM; $CaCl_2$, 0.2 mM; $MgSO_4$, 0.1 mM; HEPES, hemisodium salt, 2.5 mM; pH = 7.5) followed by centrifugation at 20,000*g* for 15 min.

Binding reactions were conducted in buffer of the following composition: NaCl, 140 mM; KCl, 1.5 mM; $CaCl_2$, 2 mM; $MgSO_4$, 1 mM; HEPES hemisodium, 25 mM; pH = 7.5. Incubations with α-Bgt also contained 0.1% bovine serum albumin.

The binding of [^{3}H]nicotine and α-Bgt was conducted as described previously (Marks et al., 1986) as modified for 100 μl incubations in 96-well microtiter plates (Marks et al., 1996). For [^{3}H]nicotine binding, samples were incubated with 17 nM [^{3}H]nicotine (K_D = 2 nM) for 30 min at 22°C. Blanks were determined by including 10 μM unlabeled nicotine in the incubation. For α-Bgt binding, samples were incubated with 2.0 nM α-Bgt (K_D = 0.5 nM) for 4 h at 22°C. Blanks were determined by including 1 mM unlabeled nicotine in the incubation.

The binding of [^{3}H]epibatidine at low concentrations (high-affinity binding) and the effect of cytisine on this binding was determined as described previously (Marks et al., 1998). Incubation volume was 500 μl. For total [^{3}H]epibatidine binding, samples were incubated with 0.36 nM [^{3}H]epibatidine (K_D = 6 pM) for 120 min at 22°C. Cytisine-resistant [^{3}H]epibatidine binding was determined by including 50 nM cytisine in the incubation. Blanks were determined by including 100 μM unlabeled nicotine in the incubation.

The binding of [^{3}H]epibatidine at high concentrations (low- plus high-affinity binding; Houghtling et al., 1995) was measured using a 100 μl incubation volume. For total [^{3}H]epibatidine, samples were incubated with 10 nM [^{3}H]epibatidine (low-affinity K_D = 6 nM) for 60 min at 22°C. Blanks were determined by including 1 mM unlabeled nicotine in the incubation. Low-affinity binding was estimated by subtracting the binding measured at 0.36 nM [^{3}H]epibatidine from that measured at 10 nM [^{3}H]epibatidine or as the amount of low-affinity binding inhibited by incubation with 300 μM dTC. The results obtained with these two calculations did not differ significantly.

At the completion of the incubations, all binding reactions were terminated by filtration using an 96-place manifold (Inotech Biosystems, Lansing, MI). Particulate fractions were collected with two glass fiber filters (top, Type GB100, Microfiltration Systems, Dublin, CA; bottom, Type A/E, Gelman Sciences, Ann Arbor, MI). Filters for collection of [^{3}H]nicotine and [^{3}H]epibatidine were treated with 0.5% polyethylenimine. GB100 filters for collection α-Bgt samples were treated with 5% nonfat skim milk dissolved in wash buffer, whereas A/E filters were treated with 0.5% polyethylenimine. Samples were washed six times. All filtrations and washes were conducted in a 4°C cold room using ice-cold buffer.

After the addition of 1 ml of Budget Solve Scintillation Fluid (Research Products International) to each sample, tritium was measured at 45% efficiency using a Packard 1600TR Liquid Scintillation Spectrometer. The ^{125}I was measured at 80% efficiency using a Packard Cobra Gamma Counter.

Protein. Protein was measured using the method of Lowry et al. (1951) with bovine serum albumin as the standard.

Data Calculation. The magnitude of agonist stimulated $^{86}Rb^+$ efflux was determined as the counts exceeding basal efflux during time of exposure to agonist. Samples were normalized to the counts remaining in the sample at the end of the stimulation period such that the signal size represented the percent of total tissue $^{86}Rb^+$ that was stimulated by agonist exposure.

Curve fitting was accomplished using the nonlinear curve fitting algorithm in Sigma Plot 5.0 (Jandel Scientific, San Rafael, CA). Concentration-effect curves were fit using either the Michaelis-Menten equation, the Hill equation, or two Michaelis-Menten equations. Relative potencies, efficacies, and regional distributions of various responses were compared using regression analysis.

Results

ACh-Stimulated $^{86}Rb^+$ Efflux. The $^{86}Rb^+$ efflux stimulated by a 5-s exposure to several concentrations of ACh is illustrated in the left panel of Fig. 1. Each point represents datum collected for a 3-s time period using a continuous flow detector. The amount of $^{86}Rb^+$ efflux increased with increasing concentrations of ACh between 1 and 1000 μM. The peak observed after stimulation with 1000 μM ACh was approximately 3-fold greater than the basal efflux. The concentration-response curve for ACh-stimulated $^{86}Rb^+$ deviated markedly from simple Michaelis-Menten kinetics (Fig. 1, right). The Hill coefficient for this curve was 0.44 $\pm$ 0.08. The results were consistent with those of a two-component process displaying EC_{50} values of 0.80 $\pm$ 0.57 μM and 82.6 $\pm$ 40.2 μM with maximal efflux representing 0.079 $\pm$ 0.019% and 0.160 $\pm$ 0.018% of total tissue $^{86}Rb^+$ during the 5-s stimulation, respectively. These results suggest that more than one process mediates ACh-stimulated $^{86}Rb^+$ efflux from mouse brain synaptosomes.

Effects of DHβE and α-Bgt. The effects of the nicotinic antagonists DHβE and α-Bgt on $^{86}Rb^+$ efflux stimulated by either 30 or 1000 μM ACh were evaluated in an attempt to pharmacologically differentiate the putative multiple processes underlying ACh-stimulated $^{86}Rb^+$ efflux from mouse brain synaptosomes (Fig. 2). Samples were treated with DHβE, an antagonist that is somewhat selective for α4/β2 nicotinic receptors, for 8 min or with α-Bgt, an antagonist that is selective for neuronal α7 nicotinic receptors, for 70 min before stimulation with ACh. The main panel on the left side of Fig. 2 presents data from representative perfusion profiles obtained with a 5-s stimulation with 30 μM ACh without antagonist treatment, and after treatment with 2 μM DHβE, 100 nM α-Bgt, or both antagonists. DHβE treatment inhibited ACh-stimulated $^{86}Rb^+$ efflux approximately 75%, whereas α-Bgt treatment had no significant effect. α-Bgt also had no additional effect in the presence of DHβE

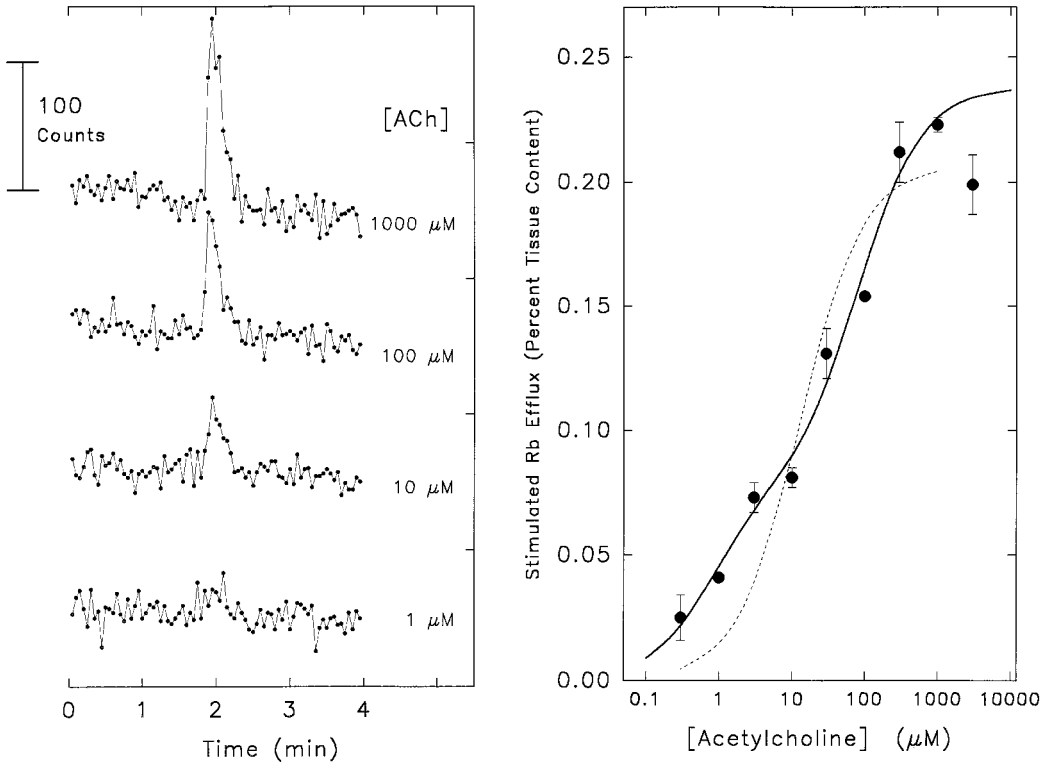

Fig. 1. Stimulation of $^{86}Rb^+$ efflux by ACh. Crude whole brain synaptosomes stimulated for 5 s with ACh. The traces (left) are actual data obtained at the indicated concentrations of ACh. Each point represents the counts measured during the 3-s sampling period. Basal efflux for each condition was approximately 50 counts per fraction. The ACh concentration-effect curve is shown in the right panel. Each point represents the mean ± S.E.M. of six determinations from three separate experiments. The curve is that obtained for a two-site fit of the data.

(Fig. 2, left, inset). The main panel on the right side of Fig. 2 presents data from representative perfusion profiles obtained with a 5-s stimulation with 1000 μM ACh. The response was inhibited approximately 40% by 2 μM DHβE, but was unaffected by 100 nM α-Bgt alone or in combination with DHβE. These results indicate that a significant fraction of ACh-stimulated $^{86}Rb^+$ efflux is sensitive to inhibition by DHβE, but not by α-Bgt. Furthermore, the DHβE-sensitive component was the same (0.8% of tissue content) whether the samples were stimulated with 30 or 1000 μM ACh.

DHβE Inhibition. The partial inhibition of ACh-stimulated $^{86}Rb^+$ efflux by 2 μM DHβE and the difference in the magnitude of this effect at different ACh concentrations suggests that this antagonist may differentially inhibit subsets of responses. Thus, the inhibitory effects of DHβE were examined by constructing concentration-response curves for responses stimulated by 30 or 1000 μM ACh (Fig. 3). Samples were exposed to DHβE for 8 min before stimulation and DHβE was present during and after the 5-s stimulation with ACh. DHβE produced a concentration-dependent decrease in $^{86}Rb^+$ efflux at both concentrations of ACh. An apparently monophasic inhibition was observed for samples stimulated with 30 μM ACh with an estimated IC_{50} value of 0.17 ± 0.02 μM. Higher concentrations of DHβE were required to inhibit $^{86}Rb^+$ efflux stimulated by 1000 μM ACh. Inasmuch as DHβE is a competitive antagonist, the shift in the concentration-effect curve could have arisen merely because of the increased ACh concentration. Inhibition by DHβE was reversible (k = 0.021/s, $T_{1/2}$ = 33 s), however with this dissociation rate, reversal of inhibition was approximately 5% during the 5-s stimulation.

When the results obtained with 30 μM ACh were subtracted from those obtained with 1000 μM ACh, the curve displayed in the inset of Fig. 3 was generated. The IC_{50} value estimated for this component was 2.6 ± 0.6 μM.

Differential DHβE inhibition curves were also generated using (−)-nicotine (10 and 300 μM) and (±)-epibatidine (0.3 and 10 μM) as agonists. Apparent IC_{50} values of 0.27 ± 0.03 and 0.28 ± 0.04 μM at the lower concentrations and 7.2 ± 3.2 and 11.8 ± 3.0 μM for the difference between the higher and lower concentrations were calculated for nicotine and epibatidine, respectively. These results suggest the existence of a relatively high-affinity, DHβE-sensitive nicotinic response and a relatively low-affinity, DHβE-resistant nicotinic response for ACh, nicotine, and epibatidine.

Stimulation of DHβE-Sensitive and DHβE-Resistant $^{86}Rb^+$ Efflux by Nicotinic Agonists. The existence of ACh-stimulated responses that are differentially sensitive to inhibition by DHβE was used to evaluate the concentration dependence of nicotinic agonist-stimulated $^{86}Rb^+$ efflux. Concentration-effect curves for ACh activation of $^{86}Rb^+$ efflux from mouse forebrain were constructed with either 0 or 2 μM DHβE present in the perfusion buffer and are shown in Fig. 4. Similar to the results presented in Fig. 1, $^{86}Rb^+$ efflux stimulated by ACh displayed a biphasic concentration-effect curve with estimated EC_{50} values of 5.4 ± 4.7 and 244 ± 328 μM and efflux of 0.12 ± 0.05 and 0.16 ± 0.05%, respectively. However, at concentrations higher than 1 mM the responses decreased. In the presence of 2 μM DHβE, a monophasic concentration-effect curve with an EC_{50} value of 540 ± 60 μM and maximal efflux of 0.16 ± 0.01% was obtained. These parameters are comparable to the low-affinity component of the full concentration-effect curve in the absence of DHβE. The difference in response between total ACh-stimulated efflux and that observed in the presence of 2 μM DHβE is shown in the inset to Fig. 4. At ACh concentrations at or below 1000 μM, the ACh-stimulated $^{86}Rb^+$ efflux appeared to be a monophasic process with an EC_{50} of 7.5 ± 2.6 μM and a maximal efflux of 0.15 ± 0.01%. These parameters are comparable to the high-affinity component of the full dose-re-

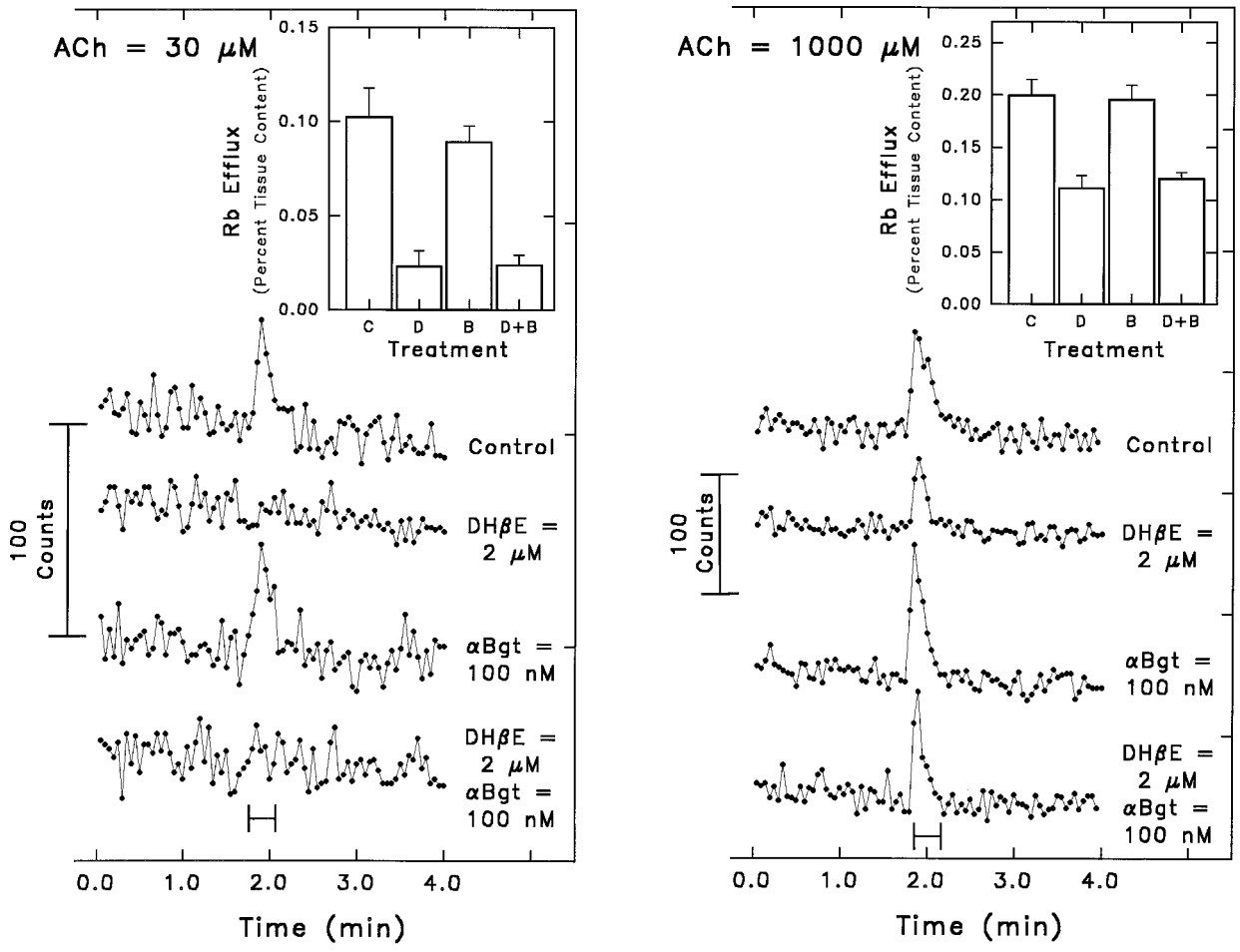

Fig. 2. Effect of 2 μM DHβE and 100 nM α-Bgt on $^{86}Rb^+$ efflux stimulated by 30 or 1000 μM ACh. The main panel of each figure illustrates primary data collected from samples of crude whole-brain synaptosomes stimulated with 30 μM ACh (left) or 1000 μM ACh (right) in the presence of 2 μM DHβE, 100 nM α-Bgt, or both agents, as indicated. Samples were stimulated with ACh for 5 s. Samples were treated with DHβE for 8 min before stimulation and with α-Bgt for 70 min before stimulation. DHβE and α-Bgt were present before, during, and after exposure to ACh. The insets summarize the responses (mean ± S.E.M., $n = 6$) obtained under each experimental condition: C, control; D, 2 μM DHβE; B, 100 nM α-Bgt; D+B, 2 μM DHβE plus 100 nM α-Bgt.

sponse curve in the absence of DHβE. Also note that a substantial decrease in efflux occurred at concentrations above 1 mM. These results indicate that differential inhibition by DHβE is a useful tool to study agonist stimulation of $^{86}Rb^+$ efflux.

Differential DHβE inhibition was used to evaluate the stimulation of $^{86}Rb^+$ efflux by 17 nicotinic agonists (Fig. 5). Most agonists elicited an increase in both DHβE-sensitive and DHβE-resistant $^{86}Rb^+$ efflux, but substantial differences in both potency and efficacy were observed (Table 1).

The EC_{50} values for activation of the DHβE-sensitive $^{86}Rb^+$ efflux were all substantially lower than the EC_{50} values for activation of DHβE-resistant $^{86}Rb^+$ efflux. However, the relative potency observed for the DHβE-sensitive and DHβE-resistant responses varied among the agonists. Many of the agonists (ACh, L-nicotine, (±)-epibatidine, (+)-epibatidine, (−)-epibatidine, methylcarbachol, and epiboxidine) were 40- to 150-fold more potent for the DHβE-sensitive response. However, DMPP, TMA, carbachol, nornicotine, and anatoxin-a exhibited less selectivity between the two responses with potency ratios of about 20. Two weak agonists, cytisine and D-nicotine, displayed large differences in potency. A-85380 was unique in that this compound stimulated substantial $^{86}Rb^+$ efflux and also displayed a large difference in potency (about 2500-fold) between the DHβE-sensitive and DHβE-resistant responses.

The agonists tested also differed considerably in the maximal responses that were measured. Furthermore, the maximal efflux observed for a given agonist for the DHβE-sensitive response could be larger than, similar to, or smaller than the maximal efflux observed for the DHβE-resistant response. Maximal $^{86}Rb^+$ efflux measured for the endogenous transmitter, ACh, was very similar for the DHβE-sensitive and DHβE-resistant responses, as was the maximal efflux for L-nicotine. Epibatidine, epiboxidine, and A-85380 elicited considerably more DHβE-resistant efflux, as did cytisine. However, cytisine was not particularly efficacious for either component. Three quaternary agonists, carbachol, DMPP, and TMA, elicited 1.6- to 5-fold greater DHβE-sensitive response than DHβE-resistant response. No detectable DHβE-resistant $^{86}Rb^+$ efflux was elicited by anabasine.

The relative potency and efficacy of the seventeen nicotinic agonists for the DHβE-sensitive and DHβE-resistant responses were compared by regression analysis (Fig. 6). The correlations between both potency and efficacy of the agonists were statistically significant ($r = 0.75$ and $r = 0.74$,

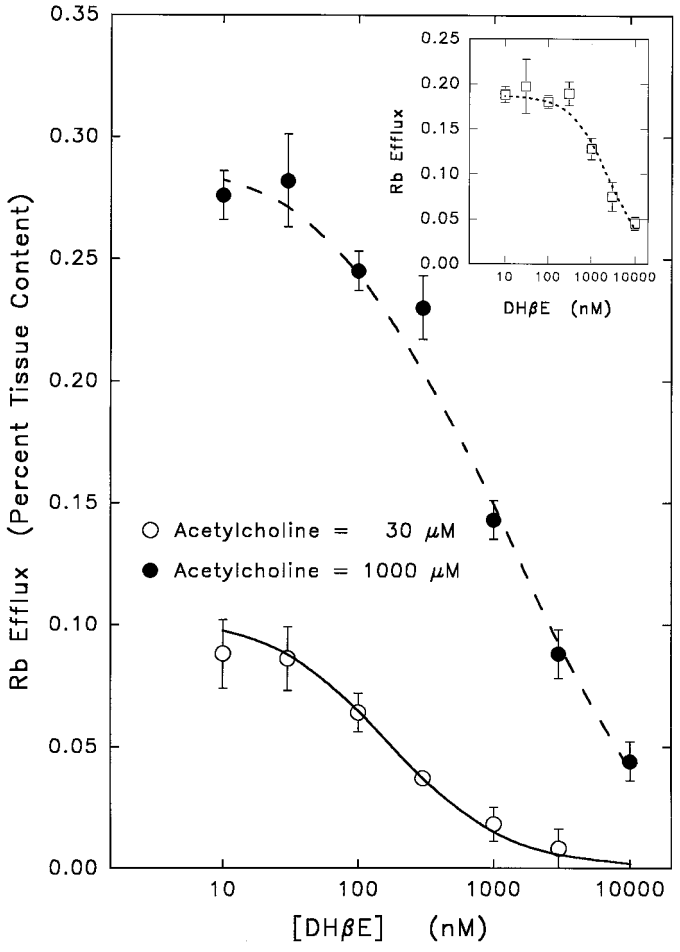

Fig. 3. Inhibition of ACh-stimulated $^{86}Rb^+$ efflux by DHβE. Crude whole-brain synaptosomes were stimulated with 30 μM ACh (○) or 1000 μM ACh (●) for 5 s after an 8-min exposure to the indicated concentrations of DHβE. The inset displays the difference in response at 1000 μM and 30 μM ACh. Each data point represents the mean ± S.E.M. of eight determinations from four separate experiments.

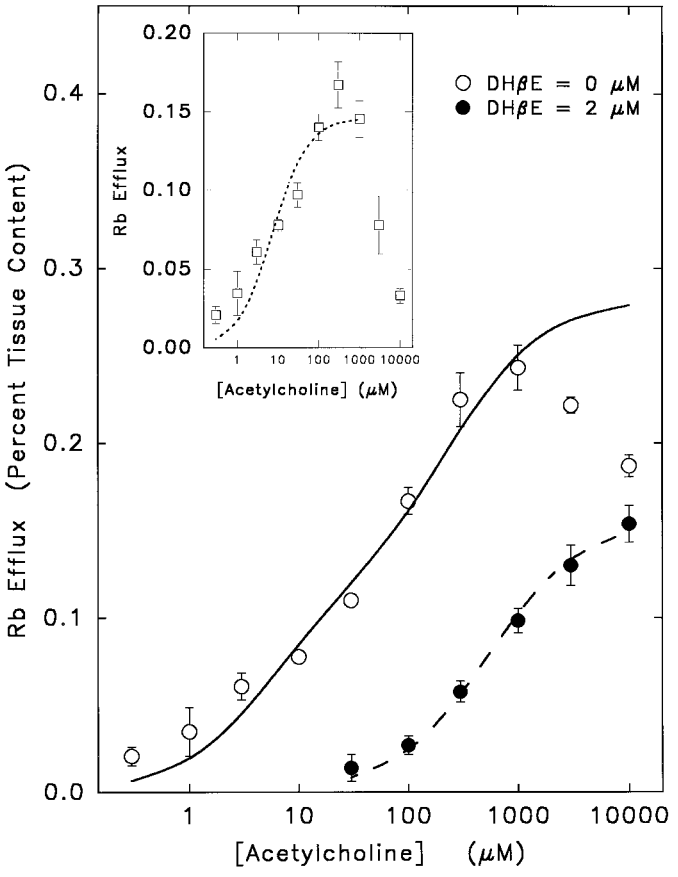

Fig. 4. Concentration-response curves for ACh in the presence of 0 or 2 μM DHβE. Crude whole-brain synaptosomes were treated with 0 μM DHβE (○) or 2 μM DHβE (●) for 8 min before a 5-s exposure to the indicated concentrations of ACh. Each point represents the mean ± S.E.M. for six determinations from three separate experiments. The inset displays the difference between the results in the absence or presence of DHβE. Curves shown for the response in the presence of DHβE and the inset are theoretical fits of the data to the Michaelis-Menten equation. The curve for the response in the absence of DHβE is a two-site fit of these data.

respectively; $p < .05$), indicating a general correspondence between these two parameters for the DHβE-sensitive and DHβE-resistant responses. However, these relationships are not particularly strong. For example, the six agonists with EC_{50} values of about 100 μM for stimulation of DHβE-resistant $^{86}Rb^+$ efflux have EC_{50} values that differ by approximately 1000-fold for the DHβE-sensitive efflux. Furthermore, the five agonists with EC_{50} values around 10 μM for DHβE-sensitive $^{86}Rb^+$ efflux have EC_{50} values that differ approximately 100-fold for the DHβE-resistant response. Similar incongruities exist for maximal efflux (E_{max}), as well.

Effects of Nicotinic Antagonists. Inhibition of DHβE-sensitive (measured with 10 μM nicotine) and DHβE-resistant (measured with 10 μM epibatidine plus 2 μM DHβE) nicotinic responses by six antagonists was studied. Concentration-effect curves for these antagonists are shown in Fig. 7 and IC_{50} values are summarized in Table 2. In contrast to the agonist effects, where every agonist was more potent in stimulating DHβE-sensitive $^{86}Rb^+$ efflux, the antagonists were not uniformly more potent inhibitors of DHβE-sensitive response. Results obtained for DHβE under these conditions confirm the differential effect of DHβE. An IC_{50} value of 0.15 ± 0.05 μM was calculated for DHβE-sensitive efflux and an IC_{50} value of 8.3 ± 1.7 μM or 13.7 ± 3.3 was calculated for the response stimulated by 10 μM epibatidine in the presence of 2 μM DHβE or 2 μM MLA, respectively. MLA is also a more potent inhibitor of DHβE-sensitive efflux (IC_{50} = 0.20 ± 0.09 μM) than it is of the DHβE-resistant response (IC_{50} = 4.4 ± 1.6 μM). Decamethonium inhibited both responses with equal potency (IC_{50} = 4.1 μM). Mecamylamine and dTC were slightly more potent inhibitors of the DHβE-resistant efflux (IC_{50} = .16 ± 0.03 μM and 1.1 ± 0.2 μM, respectively) than of the DHβE-resistant efflux (IC_{50} = .59 ± 0.09 and 2.8 ± 0.7 μM, respectively). Hexamethonium was a significantly more potent inhibitor of the DHβE-resistant response (IC_{50} = .89 ± 0.17 μM) than the DHβE-sensitive (IC_{50} = 17.6 ± 6.1 μM). Thus, all six nicotinic antagonists inhibited both DHβE-sensitive and DHβE-resistant $^{86}Rb^+$ efflux, but the relative potency of the compounds as inhibitors of the two processes varied markedly.

Responses in β2 Mutant Mice. Analysis of responses of mice expressing mutant nicotinic receptors provides one means by which the molecular basis of nicotinic responses can be investigated. The effect of null mutation of the β2 nAChR subunit on DHβE-sensitive and DHβE-resistant $^{86}Rb^+$ efflux was determined. Perfusion profiles for $^{86}Rb^+$

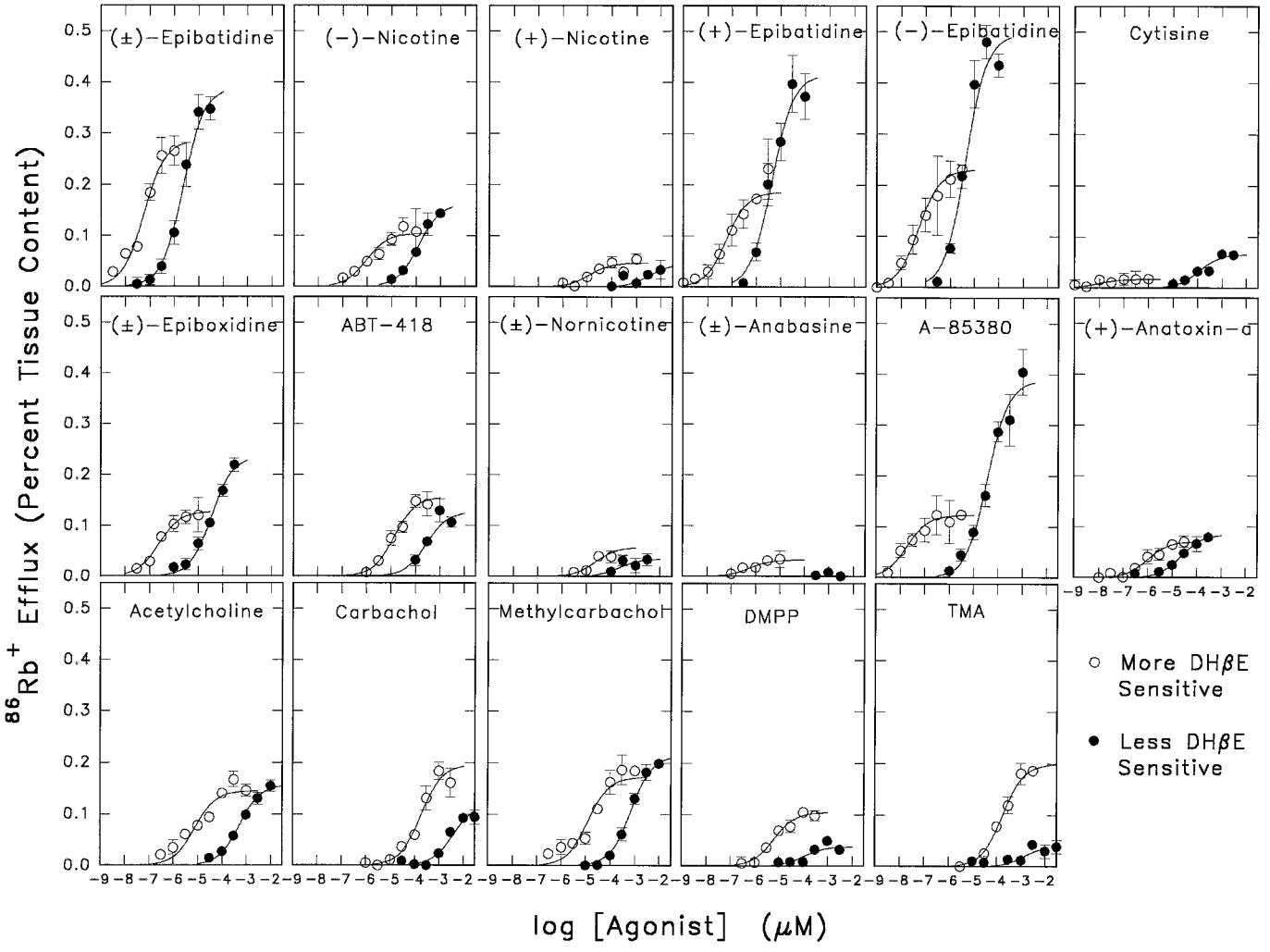

Fig. 5. Agonist simulation of DHβE-sensitive and DHβE-resistant $^{86}Rb^+$ efflux. Crude whole brain synaptosomes were stimulated with the indicated concentrations of each agonist in the presence or absence of 2 μM DHβE. Data points represent results obtained in the presence of 2 μM DHβE (●; DHβE-resistant) or the difference between the response measured in the absence or presence of 2 μM DHβE (○; DHβE-sensitive). Each point represents the mean ± S.E.M. of six to eight determinations from three to four separate experiments. Curves are theoretical fits of the data to the Michaelis-Menten equation.

efflux stimulated by a 5-s exposure to 10 μM nicotine for β2 homozygote wild type, heterozygote, and homozygote mutant mice are shown in Fig. 8 (top left). Although exposure to nicotine produced substantial increases in $^{86}Rb^+$ efflux from whole brain synaptosomes of wild type and heterozygote mice, little response was observed in the homozygote mutants. The effect of β2 genotype is summarized in Fig. 8 (bottom left). A small decrease (12%) in response was observed for the heterozygotes, but $^{86}Rb^+$ efflux stimulated by 10 μM nicotine decreased 96% in the β2 null mutants. The efflux remaining in the homozygote mutants was not significantly different from zero.

Perfusion profiles for $^{86}Rb^+$ efflux stimulated by 10 μM epibatidine in the presence of 2 μM DHβE for β2 homozygote wild type, heterozygote, and homozygote mutant mice are shown in Fig. 8 (top right). Although exposure to epibatidine in the presence of DHβE resulted in marked stimulation of $^{86}Rb^+$ efflux for both wild type and heterozygote mice, the response observed for homozygote mutants was substantially reduced. The effect of genotype on the DHβE-resistant response is summarized in Fig. 8 (bottom right). The average signal observed for β2 heterozygote mice was 29% lower than that measured for wild type mice, a significant decrease in response. DHβE-resistant $^{86}Rb^+$ efflux measured in the homozygote mutant mice was 4% of that measured for the homozygote wild type mice and was not significantly different from zero. Therefore, the β2 subunit is required for most, if not all, of the receptors that mediate both DHβE-sensitive and DHβE-resistant components of nAChR-mediated $^{86}Rb^+$ efflux.

Distribution of DHβE-Sensitive and DHβE-Resistant $^{86}Rb^+$ Efflux in Mouse Brain. The experiments described above were performed using crude synaptosomes prepared from whole mouse forebrain. To determine the distribution of DHβE-sensitive and DHβE-resistant nicotinic responses throughout the brain, $^{86}Rb^+$ efflux stimulated by 10 μM nicotine or 10 μM epibatidine in the presence of 2 μM DHβE was measured in crude synaptosomes prepared from 15 brain areas. The results of these experiments are shown in Fig. 9.

The amount of $^{86}Rb^+$ efflux stimulated by 10 μM nicotine (DHβE-sensitive) varied substantially among brain regions (Fig. 9, top left). The least efflux was observed in Cb. Low

TABLE 1
EC_{50} values and maximal efflux rates for DHβE-sensitive and DHβE-resistant $^{86}Rb^+$ efflux

Agonist	DHβE-Sensitive Response		DHβE-Resistant Response	
	EC_{50}	E_{max}	EC_{50}	E_{max}
	μM	%	*μM*	%
A85380	0.018 ± .006	0.120 ± .006	40.0 ± 8.5	0.392 ± .020
ABT418	12.6 ± 3.4	0.153 ± .010	277 ± 150	0.134 ± .020
Acetylcholine	7.18 ± .29	0.149 ± .011	550 ± 61	0.158 ± .005
Anabasine	52.9 ± 23.9	0.035 ± .004	No Response	No Response
Anatoxin-a	0.96 ± .26	0.070 ± .004	23.8 ± 4.5	0.084 ± .004
Carbachol	150 ± 40	0.188 ± .013	2600 ± 830	0.109 ± .010
Cytisine	0.013 ± .011	0.017 ± .003	150 ± 60	0.068 ± .007
DMPP	6.1 ± 1.4	0.102 ± .005	160 ± 110	0.043 ± .008
(±)-Epibatidine	0.057 ± .016	0.289 ± .019	2.2 ± 0.3	0.392 ± .017
(+)-Epibatidine	0.093 ± .029	0.211 ± .015	3.8 ± 0.9	0.410 ± .024
(−)-Epibatidine	0.049 ± .008	0.223 ± .007	3.7 ± 1.1	0.498 ± .034
Epiboxidine	0.23 ± .04	0.125 ± .004	32.3 ± 6.2	0.236 ± .013
Methylcarbachol	19.4 ± 5.4	0.192 ± .012	730 ± 80	0.218 ± .007
(−)-Nicotine	1.39 ± .42	0.112 ± .007	130 ± 20	0.164 ± .007
(+)-Nicotine	13.4 ± 8.6	0.047 ± .006	1200 ± 330	0.035 ± .012
Nornicotine	17.7 ± 13.1	0.050 ± .013	190 ± 190	0.034 ± .009
TMA	185 ± 32	0.203 ± .009	890 ± 720	0.040 ± .007

Kinetic values for the activation of both DHβE-sensitive and DHβE-resistant $^{86}Rb^+$ efflux from mouse forebrain synaptosomes were calculated by nonlinear least squares curve fitting of the results shown in Fig. 5 using the Michaelis-Menten equation. Values given are mean ± S.E.M. of the estimates obtained for results of at least three separate experiments. E_{max} values are the percentage of total synaptosomal $^{86}Rb^+$ stimulated by agonist exposure.

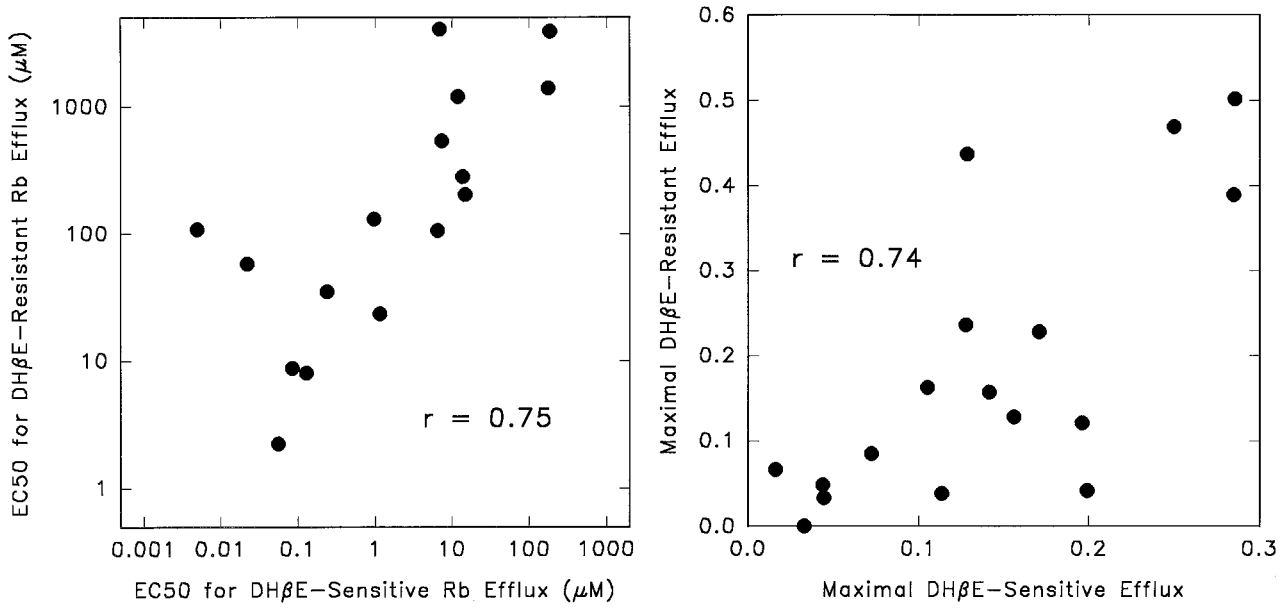

Fig. 6. Correlations between EC_{50} values and maximal efflux for DHβE-sensitive and DHβE-resistant $^{86}Rb^+$ efflux. EC_{50} values (left) and maximal efflux (right) determined for the agonist curves of Fig. 5 for the DHβE-sensitive response are compared to the corresponding values for the DHβE-resistant response.

levels were also observed in OB and Se. The largest nicotine-stimulated efflux was observed in Th. High levels were also measured for IPN and Hab.

The amount of $^{86}Rb^+$ efflux stimulated by 10 μM epibatidine in the presence 2 μM DHβE (DHβE-resistant) also varied substantially among brain regions (Fig. 9, bottom left). The lowest DHβE-resistant efflux was measured in Cb and Se, whereas the greatest DHβE-resistant response was measured in SC and Th.

The regional distribution of the DHβE-sensitive $^{86}Rb^+$ efflux was compared to that for the DHβE-resistant response as shown in Fig. 9 (right). The efflux stimulated by 10 μM nicotine is significantly correlated to that stimulated by 10 μM epibatidine plus 2 μM DHβE ($r = 0.86$, df = 13, $p < .05$) indicating that regional distribution of these two responses is similar. However, the relative amount of DHβE-resistant efflux measured in SC, IC, MB, and HB is substantially greater than that predicted from the amount of DHβE-sensitive efflux observed in these regions.

Comparison of nAChR-Mediated $^{86}Rb^+$ Efflux to Nicotinic Binding Sites. Because the pharmacological properties, and to a lesser extent the regional distribution, of the DHβE-sensitive response differ from those of the DHβE-resistant response, a comparison of the distribution of the functional responses to that of nicotinic binding sites may indicate a relationship between binding and function. Several nicotinic binding sites can be measured using radioligand binding assays. High-affinity [^{3}H]nicotine binding and α-Bgt binding have been used to measure two distinct binding sites (Marks et al., 1986). Recently the binding of [^{3}H]epi-

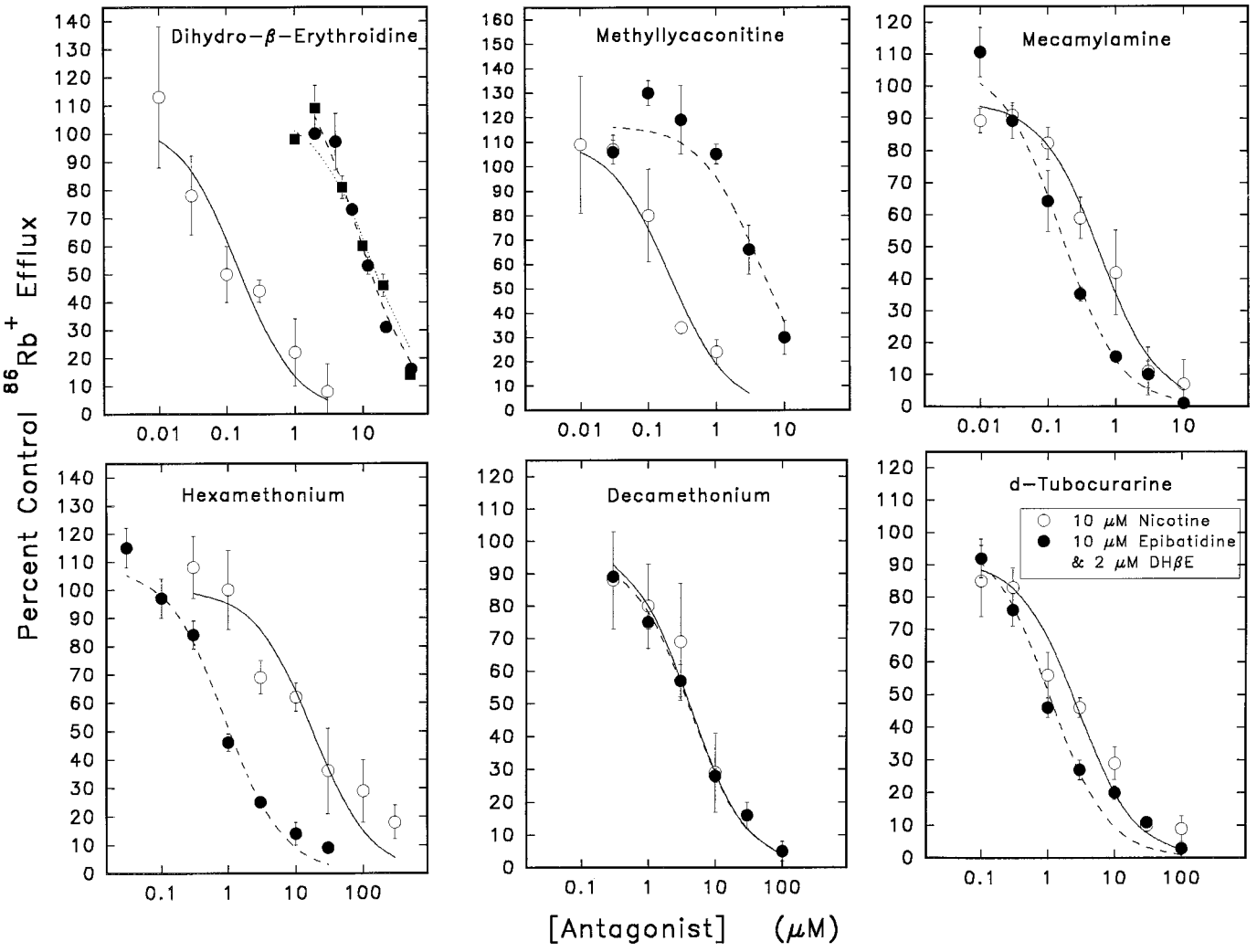

Fig. 7. Inhibition of DHβE-sensitive and DHβE-resistant $^{86}Rb^+$ efflux by nicotinic antagonists. Crude whole-brain synaptosomes were exposed to the indicated concentration of antagonists for 8 min before a 5-s exposure to 10 μM L-nicotine (○) or 10 μM (±)-epibatidine plus 2 μM DHβE (●). Those samples to be stimulated with (±)-epibatidine were treated with 2 μM DHβE as well as the test antagonist for 8 min before stimulation. In a separate set of of experiments, samples for which DHβE inhibition of the DHβE-resistant response were measured were treated with 2 μM MLA (■) instead of DHβE to allow analysis of DHβE inhibition in the absence of this antagonist. Each point represents the mean ± S.E.M. of six to eight individual measurements from three to four separate experiments. The curves are theoretical one-site fits using the equation: $A_I = 100/(1+(I/IC_{50}))$, where A_I is the percentage of control activity at antagonist concentration, I, and IC_{50} is the antagonist concentration that gives 50% inhibition.

TABLE 2

IC_{50} values for inhibition of DHβE-sensitive and DHβE-resistant $^{86}Rb^+$ efflux

Antagonist	DHβE-Sensitive Response IC_{50}	DHβE-Resistant Response IC_{50}
	μM	*μM*
Decamethonium	4.1 ± 1.7	4.1 ± 0.4
DHβE	0.15 ± .05	8.3 ± 1.7 (DHβE)
		13.7 ± 3.3 (MLA)
Hexamethonium	16.6 ± 6.1	0.89 ± .17
Mecamylamine	0.59 ± .09	0.16 ± .03
MLA	0.20 ± .06	4.4 ± 1.6
dTC	2.8 ± .7	1.1 ± .2

IC_{50} values were calculated by nonlinear least squares curve fits of the results shown in Fig. 7 using the equation: $R = R_0/(1 + I/IC_{50})$. The DHβE-sensitive response was measured for samples stimulated with 10 μM (−)-nicotine. The DHβE-resistant response was measured for samples stimulated with 10 μM (±)-epibatidine in the presence of 2 μM DHβE. IC_{50} values for DHβE were also measured using 2 μM MLA. Values are mean ± S.E.M. estimated from the curve fits.

batidine has been characterized (Houghtling et al., 1995). This ligand measures several nicotinic binding sites: a high-affinity site sensitive to inhibition by cytisine (identical with the high-affinity agonist site), a high-affinity site relatively resistant to inhibition by cytisine and that may include more than one site, and a low-affinity site (Houghtling et al., 1995; Marks et al., 1998; Zoli et al., 1998).

The properties of [^{3}H]epibatidine binding to whole mouse brain are illustrated in Fig. 10. The saturation curve for [^{3}H]epibatidine binding is shown in Fig. 10 (top). The binding isotherm deviates from that of a single site, as illustrated by the biphasic Scatchard plot shown in the inset to this panel. The binding constants for the two components as estimated from nonlinear least-squares fitting of the primary data were K_D of 0.020 ± 0.004 nM and B_{max} of 98 ± 4 fmol/mg protein for the high-affinity site and K_D of 6.4 ± 2.8 nM and B_{max} of 65 ± 7 fmol/mg protein for the low-affinity site. The inhibition of [^{3}H]epibatidine binding at two ligand concentrations by cytisine and dTC was used to further evaluate the properties of the sites. Fig. 10 (bottom left) displays the results for cytisine inhibition. At a [^{3}H]epibatidine concentration of 0.44 nM, when the high-affinity site is fully saturated with little

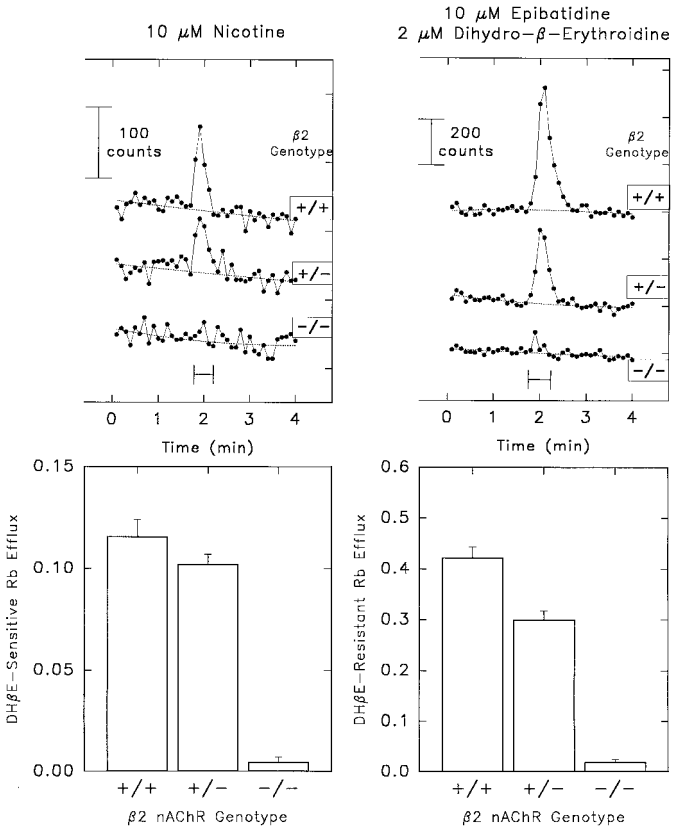

Fig. 8. Effect of β2 genotype on DHβE-sensitive and DHβE-resistant $^{86}Rb^+$ efflux. Crude synaptosomes were prepared from whole brains of mice with the following genotype for the β2 nAChR subunit: +/+, homozygote wild type; ±, heterozygote; −/−, homozygote mutant. The top panels illustrate primary data for mice of each genotype receiving a 5-s stimulation with 10 μM L-nicotine (left) or 10 μM (±)-epibatidine plus 2 μM DHβE (right). DHβE was present before, during, and after the stimulation with epibatidine. The bottom panels summarize data (mean ± S.E.M.) obtained for four wild type, seven heterozygote, and five mutant mice.

binding at the low-affinity site, inhibition by cytisine is biphasic. Approximately 85% of the binding was sensitive to cytisine (IC_{50} = 6.7 nM, estimated K_I = .26 nM) with the remaining 15% of the binding relatively resistant to cytisine (IC_{50} = 340 nM, estimated K_I = 13 nM). At a [^{3}H]epibatidine concentration of 12.5 nM, where both high- and low-affinity binding occurs, the pattern of cytisine inhibition was not markedly different from that observed at 0.44 nM. Inhibition of the low-affinity site was estimated and is illustrated in the inset to the bottom left panel. The binding parameters estimated were an IC_{50} value of 1.8 ± 0.3 (estimated K_I = .59 μM) with a initial binding of 49 ± 2 fmol/mg protein. The similarity of the ratios of cytisine K_I values for the high- and low-affinity sites (~15- and ~95-fold for the high- and low-affinity [^{3}H]epibatidine binding sites, respectively) underlies the inability of cytisine inhibition to distinguish these sites. Fig. 10 (bottom right) demonstrates the inhibition of [^{3}H]epibatidine binding by dTC. With a [^{3}H]epibatidine concentration of 0.44 nM, inhibition by dTC is biphasic, similar to the biphasic inhibition obtained with cytisine. Approximately 87% of the sites were sensitive to inhibition by dTC (IC_{50} = 49 ± 10 μM, estimated K_I = 2.2 μM), whereas the remaining 13% of the sites were less sensitive (IC_{50} = 1500 ± 1400 μM, estimated K_I = 64 μM). With 12.5 nM [^{3}H]epibatidine, the inhibition by dTC was substantially different than that by cytisine in that approximately one-third of the binding was inhibited by 100 μM dTC. This fraction of the inhibition corresponded to the low-affinity binding as illustrated in the inset to the bottom right panel. The binding site parameters estimated were an IC_{50} of 12.2 ± 2.4 μM (estimated K_I = 4.1 μM) with a binding site density of 53 ± 2 fmol/mg. This low-affinity [^{3}H]epibatidine binding component was similar to that calculated with cytisine inhibition. The ability of dTC to selectively inhibit low-affinity [^{3}H]epibatidine binding was made possible because the K_I/K_D ratio was about 100,000 for the high-affinity site compared with about 650 for the low-affinity site, and the K_I values were comparable (2.1 and 4.1 μM, respectively). Thus, low-affinity [^{3}H]epibatidine binding sites were estimated by selective dTC inhibition at a high ligand concentration (about 10 nM), and cytisine-resistant sites were estimated by selective cytisine inhibition at a low ligand concentration (about 0.5 nM).

[^{3}H]Nicotine, α-Bgt, and three [^{3}H]epibatidine binding sites were measured in P2s prepared from fifteen regions of mouse brain for comparison to the amount of DHβE-sensitive and DHβE-resistant $^{86}Rb^+$ efflux measured in these regions (Fig. 11). Correlational analyses indicate that neither cytisine-resistant high-affinity epibatidine binding nor α-Bgt binding have regional distributions similar to those for the two functional responses. However, significant correlations between functional response and high-affinity nicotine binding as well as between functional response and low-affinity epibatidine binding were observed. The two highest correlation coefficients were observed for nicotine binding and DHβE-sensitive $^{86}Rb^+$ efflux (r = 0.94) and for low-affinity epibatidine binding and DHβE-resistant $^{86}Rb^+$ efflux (r = 0.94). The correlations between nicotine binding and DHβE-resistant $^{86}Rb^+$ efflux and low-affinity epibatidine binding and DHβE-sensitive $^{86}Rb^+$ efflux were also significant (r = 0.87 and r = 0.85, respectively).

Discussion

Two pharmacologically distinct components of nicotinic agonist-stimulated $^{86}Rb^+$ efflux from mouse brain synaptosomes were analyzed using an online continuous flow radioactivity monitor. Differential sensitivity to inhibition by the nicotinic antagonist DHβE was exploited to study the pharmacology and regional distribution of these responses. The efflux inhibited by low concentrations of DHβE displayed a higher affinity for nicotinic agonists than did the response that was less sensitive to DHβE inhibition. Both the DHβE-sensitive and DHβE-resistant components were reduced more than 95% in β2 null mutant mice, revealing an absolute requirement for this subunit. The DHβE-sensitive and DHβE-resistant responses were widely distributed throughout the brain with similar, but not identical, regional distribution. Thus, a novel DHβE-resistant functional nicotinic response is widely distributed in mouse brain. This response is robust and pharmacologically distinct from those characterized previously. Whether this response is mediated by a single receptor subtype remains to be determined.

Differential inhibition by DHβE was used to measure the two pharmacologically distinct nicotinic responses. Because DHβE is a competitive antagonist, the DHβE-resistant response may have occurred because inhibition was overcome

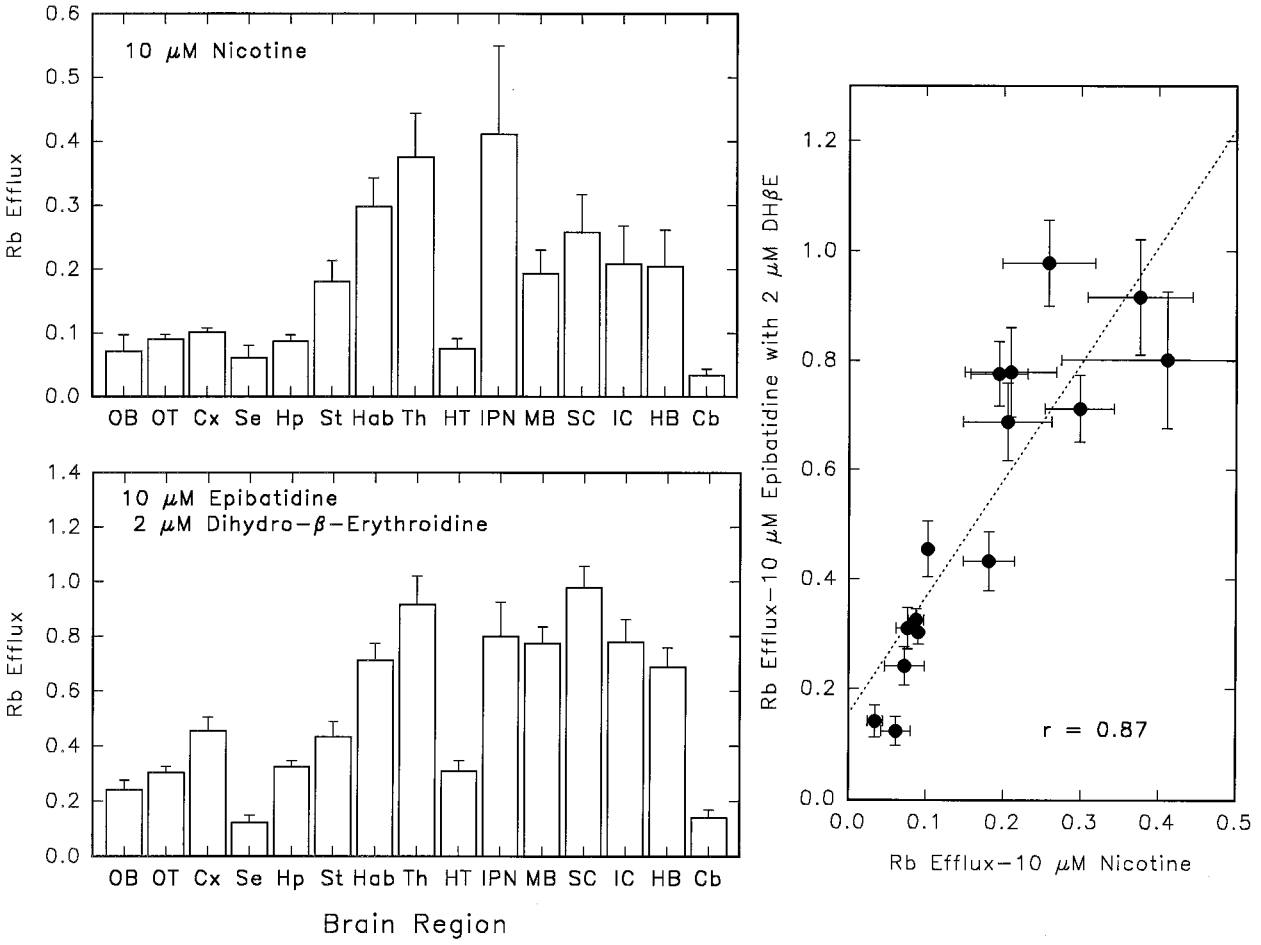

Fig. 9. DHβE-sensitive and DHβE-resistant $^{86}Rb^+$ efflux in 15 brain regions. Crude synaptosomes were prepared from the following brain regions: OB, OT, Cx, Se, Hp, St, Hab, Th, HT, IPN, MB, SC, IC, HB, Cb. $^{86}Rb^+$ efflux was stimulated by a 5-s exposure to 10 μM nicotine (top left) or 10 μM epibatidine plus 2 μM DHβE (bottom left). DHβE was present before, during, and after stimulation with DHβE. Values represent mean ± S.E.M. of four separate experiments. The magnitude of the DHβE-resistant response is compared to the magnitude of the DHβE-sensitive response in the right panel.

at high agonist concentrations. To reduce agonist-dependent changes in IC_{50} values and subsequent changes in the amount of inhibition, samples were treated with DHβE before stimulation. Therefore, reversal of blockade requires dissociation of bound DHβE. Although dissociation is relatively rapid (k = 0.02 sec^{-1}), little reversal (about 5%) of inhibition would occur during the 5-s stimulation. Thus, under the conditions used in these experiments, differential inhibition by DHβE appears to be a valid experimental approach to resolve different nicotinic responses.

Differential sensitivity of nicotinic agonist-stimulated responses to inhibition by DHβE is not a unique observation. Pharmacologically distinct nicotinic responses in hippocampal cell cultures (Alkondon and Albuquerque, 1993) and in neurons isolated from the IPN compared to neurons isolated from medial habenula (Mulle et al., 1991) displayed differential responses to DHβE inhibition. Indeed, differential DHβE sensitivity was used to investigate nAChR subtypes in hippocampal cultures (Alkondon and Albuquerque, 1995) in a manner analogous to that used in the current study. Biochemical assays of nicotinic receptor function also exhibit differential sensitivity to inhibition by DHβE. For example, nicotine-stimulated dopamine release is relatively more sensitive to inhibition by DHβE (Grady et al., 1992; Sacaan et al., 1995; Clarke and Reuben, 1996), than is nicotine-stimulated norepinephrine release (Sacaan et al., 1995; Clarke and Reuben, 1996). Defined nicotinic receptor subtypes expressed in Xenopus oocytes are differentially affected by DHβE (Harvey et al., 1996; Chavez-Noriega et al., 1997). Structural determinants for differential DHβE sensitivity are present in both α (Harvey et al., 1996) and β subunits (Harvey and Leutje, 1996).

In addition to DHβE, two antagonists, MLA and hexamethonium, differed markedly in their inhibitory potency. The selectivity demonstrated by MLA was comparable to that of DHβE. In contrast, hexamethonium was a more potent inhibitor of the DHβE-resistant response. Three other antagonists displayed similar inhibition of the DHβE-sensitive and DHβE-resistant components. Potency and efficacy for both DHβE-sensitive and DHβE-resistant $^{86}Rb^+$ efflux differed among nicotinic agonists, but every agonist tested was more potent for the DHβE-sensitive component. Differential effects of antagonists and agonists on DHβE-sensitive and DHβE-resistant $^{86}Rb^+$ efflux indicate the existence of at least two receptors.

Determining the molecular compositions of the nAChR subtypes that mediate the DHβE-sensitive and DHβE-resistant responses is important. Both DHβE-sensitive and

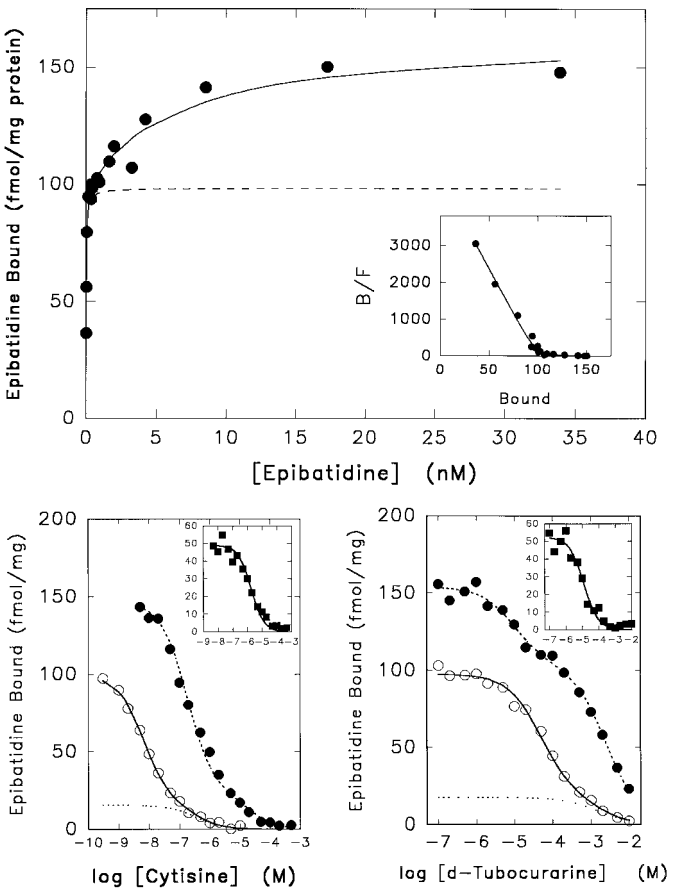

Fig. 10. [^{3}H]Epibatidine binding and inhibition by cytisine and dTC. The main top panel illustrates a representative saturation curve for the binding of [^{3}H]epibatidine to whole mouse brain particulate fraction. Actual data are represented by the points (●). The solid curve is the least-squares fit of the data to a two-site model and the dotted curve is the theoretical binding to the high-affinity site. The inset to this panel is the Scatchard plot of these data. The main panel at the bottom left displays the inhibition of [^{3}H]epibatidine binding by cytisine and the main panel at the bottom right displays the inhibition of binding by dTC at 0.44 nM (○) or 12.5 nM (●) [^{3}H]epibatidine. The solid curve at 0.44 nM [^{3}H]epibatidine is the least-squares two-site fit of the data, whereas the dotted curve presents the theoretical low-affinity binding site. The dotted curve at 12.5 nM is the least-squares two-site fit of these data. The inset to this panel is the calculated inhibition profile for the low-affinity binding site calculated as described in *Experimental Procedures*. The curve is the theoretical one-site fit of these data.

DHβE-resistant $^{86}Rb^+$ efflux were reduced more than 95% in β2-null mutant mice (Picciotto et al., 1995). Thus, both responses are nicotinic and the β2 subunit is an essential component of the nAChR mediating these responses. The identity of the α subunits remains to be unequivocally established.

In the absence of definitive assignment of subunit composition beyond the absolute requirement for β2, pharmacological and physiological data provide information about the potential subunit identity. Differences in sensitivity to agonist stimulation have been observed for other nicotinic receptors and these differences have been used to investigate potential molecular composition of the receptors. Four classical nicotinic agonists (ACh, (−)-nicotine, cytisine, and DMPP) show distinct differences in the activation of heterologously expressed receptors of defined composition (Leutje and Patrick, 1991; Chavez-Noriega et al., 1997). DHβE-sensitive $^{86}Rb^+$ efflux stimulated by these agonists most closely resembles the responses observed for the α4β2 nAChR. Several other agonists that were evaluated in the current study have also been measured in systems of defined receptor composition. The relative potency and efficacy of epibatidine (Gerzanich et al., 1995; Gopalakrishnan et al., 1996), ABT-418 (Gopalakrishnan et al., 1996), and A-85380 (Sullivan et al., 1996) measured for α4β2 nAChR are comparable to those determined for DHβE-sensitive $^{86}Rb^+$ efflux. Furthermore, the potencies and relative efficacies of ACh, anatoxin-a, cytisine, (+)-epibatidine, (−)-epibatidine, (−)-nicotine, and DMPP, for which both the Type II responses of hippocampal cells (Alkondon and Albuquerque, 1995; Zoli et al., 1998) and DHβE-sensitive $^{86}Rb^+$ efflux were determined, are comparable. The Type II response most probably is mediated by α4β2 the nAChR (Alkondon et al., 1994). Finally, the close correlation between the regional distribution of high-affinity nicotine binding and DHβE-sensitive $^{86}Rb^+$ efflux reported here and previously (Marks et al., 1993, 1996) suggests that this component is an α4β2 nAChR because high-affinity agonist binding measures primarily, if not exclusively, this subtype (Whiting and Lindstrom, 1988; Flores et al., 1992). Thus, the receptor mediating DHβE-sensitive $^{86}Rb^+$ efflux in the majority of brain regions is likely to be the α4β2 subtype, perhaps with other subunits contributing in certain brain regions.

The possible molecular structure(s) of the DHβE-resistant component is less clear. Results with null mutant mice demonstrate that the β2 subunit is required. The broad distribution of the DHβE-resistant response makes it unlikely to be mediated by receptors containing either α2 or α3 nAChR subunits because the mRNA encoding these subunits has restricted expression in rat and mouse brain (Wada et al., 1989; Marks et al., 1992). Furthermore, the poor correlation between DHβE-resistant $^{86}Rb^+$ efflux and cytisine-resistant high-affinity epibatidine binding, which may measure α3 nAChR (Marks et al., 1998; Zoli et al., 1998), suggests no relationship between the functional response and this binding component. The failure of α-Bgt or low concentrations of MLA to measurably inhibit either the DHβE-sensitive or DHβE-resistant responses indicates that α7-containing nAChRs are not involved. Considering the rapid desensitization and rundown that is displayed by α7 nAChRs, the experimental conditions used in these studies may not be well suited to measure these receptors.

The DHβE-resistant response may be mediated by a receptor with an as yet unidentified α subunit. Because subunit composition profoundly affects nAChR pharmacology and physiology (Luetje and Patrick, 1991; Chavez-Noriega et al., 1997), expression of an nAChR with an α subunit other than α4 could produce the DHβE-resistant response. If such a subunit exists, it must be widely distributed, inasmuch as the DHβE-resistant response is found throughout the brain. Receptors assembled from more than two different subunits also can display distinct pharmacology. For example, when the α5 subunit coassembles with other nAChR subunits, properties of the resulting receptor are altered (Ramirez-Latorre et al., 1996; Wang et al., 1996; Conroy and Berg, 1998). Although receptors containing α5 subunits are known, this subunit may be too sparsely expressed in rat and mouse brain to account for all of the DHβE-resistant response (Wada et al., 1990; Marks et al., 1992). The DHβE-resistant

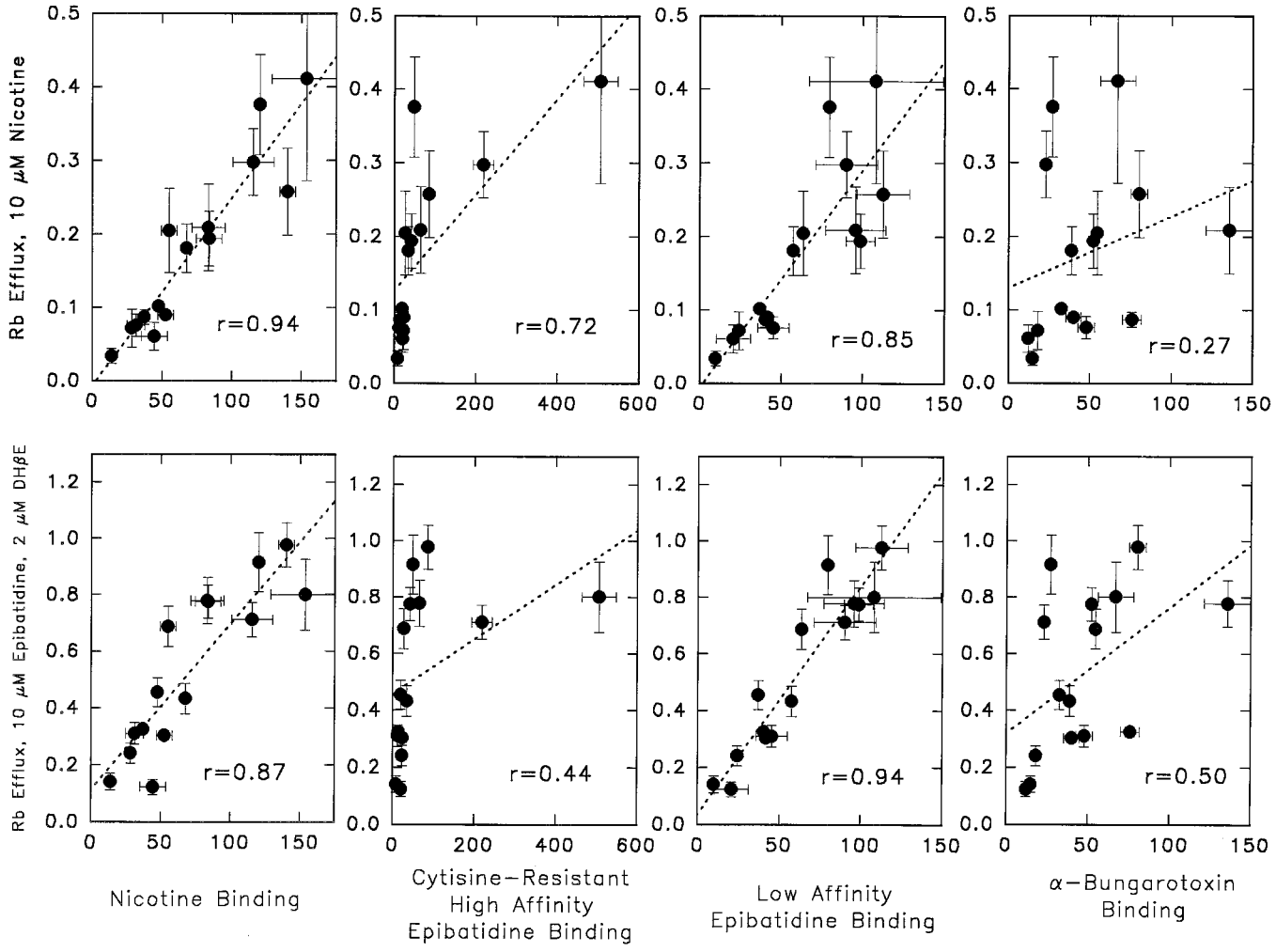

Fig. 11. Comparison of regional distribution of DHβE-sensitive or DHβE-resistant $^{86}Rb^+$ efflux to the regional distribution of nicotinic binding sites. $^{86}Rb^+$ efflux stimulated by 10 μM nicotine (top) or by 10 μM epibatidine plus 2 μM DHβE (bottom) in 15 brain regions is compared to the density of nicotinic binding sites measured with 17 nM [^{3}H]nicotine (Nicotine Binding), 0.36 nM [^{3}H]epibatidine binding in the presence of 50 nM cytisine (Cytisine-Resistant High-Affinity Epibatidine Binding), as the difference between binding of 10 nM [^{3}H]epibatidine in the absence or presence of 300 μM dTC (Low-Affinity Epibatidine Binding), or with 2 nM α-Bgt (α-Bungarotoxin Binding). Each point represents the mean ± S.E.M. of the efflux or binding in each of 15 brain regions. Correlation coefficients are displayed in each panel.

response may also be mediated by an $\alpha4\beta2$ receptor with a subunit stoichiometry other than $(\alpha4)_2(\beta2)_3$, a receptor that exists in an alternative conformational state, or a receptor that has undergone differential post-translational processing. The response might also be mediated by receptor subunits containing alternatively spliced subunits. Splice variants at the C terminus of rat α4 subunit are known (Goldman et al., 1987; Yu et al., 1996), but the properties of the subsequent nAChR formed from these variants do not differ. However, changes in the amino acids in the ligand binding domain can substantially change agonist (Corringer et al., 1998) or antagonist (Harvey et al., 1996) affinity. Splice variants with changes at or near the ligand binding sites could conceivably alter both agonist and antagonist affinity to produce the DHβE-resistant receptors.

Whatever the molecular identity of the DHβE-resistant response, it is likely to serve an important functional role. This response is expressed throughout the brain, and, if the in vitro measurements are any indication, would produce rapid, large responses. Although higher concentrations of ACh or nicotine are required to activate the DHβE-resistant response than the DHβE-sensitive response, the potency of these agonists for the DHβE-resistant response is comparable to that observed for many nAChR subtypes (Couturier et al., 1990; Gross et al., 1991; Seguela et al., 1993; Alkondon and Albuquerque, 1993; Gerzanich et al., 1995; Chavez-Noriega et al., 1997).

In summary, the experiments presented in this paper describe two components of nicotinic receptor-mediated $^{86}Rb^+$ efflux that are of similar magnitude but are differentially sensitive to inhibition to DHβE, and are predominantly, if not exclusively, composed of β2 containing nAChR. The DHβE-sensitive component appears to be identical with one described previously. The DHβE-resistant component represents a previously undescribed, but ubiquitous and robust nAChR-mediated response that may be of significant functional consequence.

References

Alkondon M and Albuquerque EX (1993) Diversity of nicotinic acetylcholine receptors in rat hippocampal neurons. I. Pharmacological and functional evidence for distinct structural subtypes. *J Pharmacol Exp Ther* **265:**1455–1473.

Alkondon M and Albuquerque EX (1995) Diversity of nicotinic acetylcholine recep-

tors in rat hippocampal neurons. III. Agonist actions of the novel alkaloid epibatidine and analysis of type II current. *J Pharmacol Exp Ther* **271:**494–506.
Alkondon M, Reinhardt S, Lorron C, Hermsen B, Maelicke A and Albuquerque EX (1994) Diversity of nicotinic acetylcholine receptors in rat hippocampal neurons. II. The rundown and inward rectification of agonist-elicited whole-cell currents and identification of receptor subunits by in situ hybridization. *J Pharmacol Exp Ther* **271:**494–506.
Brioni JD, Decker MW, Sullivan JP and Arneric SP (1997) The pharmacology of (−)-nicotine and novel cholinergic channel activators. *Adv Pharmacol* **17:**153–214.
Chavez-Noriega LE, Crona JH, Washburn MS, Urrutia A, Elliot KJ and Johnson EC (1997) Pharmacological characterization of recombinant human neuronal acetylcholine receptors hα2β2, hα2β4, hα3β2, hα3β4, hα4β2, hα4β4, and hα7 expressed in Xenopus oocytes. *J Pharmacol Exp Ther* **280:**346–356.
Clarke PBS and Reuben M (1996) Release of [^{3}H]noradrenaline from rat hippocampal synaptosomes by nicotine: Mediation by different nicotinic receptor subtypes from striatal [^{3}H]dopamine release. *Br J Pharmacol* **117:**595–606.
Conroy WG and Berg DK (1998) Nicotinic receptor subtypes in the developing chick brain: Appearance of a species containing the alpha4, beta2 and alpha5 gene products. *Mol Pharmacol* **53:**392–401.
Corringer P-J, Bertrand S, Bohler S, Edelstein SJ, Changeux J-P and Bertrand D (1998) Critical elements determining diversity of agonist binding and desensitization of neuronal nicotinic acetylcholine receptors. *J Neurosci* **18:**648–657.
Couturier S, Bertrand D, Matter J, Hernandez M, Bertrand S, Millar N, Valera S, Barkas T and Ballivet M (1990) A neuronal nicotinic acetylcholine receptor subunit (α7) is developmentally regulated and forms a homoligomeric channel blocked by α-bungarotoxin. *Neuron* **5:**847–856.
Flores CM, Rogers SW, Pabreza LA, Wolfe BB and Kellar KJ (1992) A subtype of nicotinic cholinergic receptor in rat brain is composed of α4 and β2 subunits and is up-regulated by chronic nicotine treatment. *Mol Pharmacol* **41:**31–37.
Gerzanich V, Peng X, Wang F, Wells G, Anand R, Fletcher S and Lindstrom J (1995) Comparative pharmacology of epibatidine: A potent agonist for neuronal nicotinic acetylcholine receptors. *Mol Pharmacol* **48:**774–782.
Goldman D, Deneris E, Luyten W, Kochhar A, Patrick J and Heinemann S (1987) Members of a nicotinic acetylcholine receptor gene family are expressed in different regions of the mammalian central nervous system. *Cell* **48:**965–973.
Gopalakrishnan M, Monteggia LM, Anderson DJ, Molinari EJ, Piattoni-Kaplan M, Donnelly-Roberts D, Arneric SP and Sullivan JP (1996) Stable expression, pharmacological properties and regulation of the human neuronal nicotinic acetylcholine α4β2 receptor. *J Pharmacol Exp Ther* **276:**289–297.
Grady SR, Marks MJ, Wonnacott S and Collins AC (1992) Characterization of nicotinic receptor-mediated [^{3}H]dopamine release from synaptosomes prepared from mouse striatum. *J Neurochem* **59:**848–856.
Gross A, Ballivet M, Rungger D and Bertrand D (1991) Neuronal nicotinic acetylcholine receptors expressed in Xenopus oocytes: Role of the α subunit in agonist sensitivity and desensitization. *Pfluegers Arch* **419:**545–551.
Harvey SC and Leutje CW (1996) Determinants of competitive antagonist sensitivity on neuronal nicotinic receptor beta subunits. *J Neurosci* **16:**3798–3806.
Harvey SC, Maddox FN and Leutje CW (1996) Multiple determinants of dihydro-beta-erythroidine sensitivity on rat neuronal nicotinic receptor alpha subunits. *J Neurochem* **67:**1953–1959.
Houghtling RA, Davila-Garcia MI, Hurt SD and Kellar KJ (1995) Characterization of [^{3}H]epibatidine binding to nicotinic cholinergic receptors in rat and human brain. *Mol Pharmacol* **48:**280–287.
Luetje CW and Patrick J (1991) Both α- and β-subunits contribute to the agonist sensitivity of neuronal nicotinic acetylcholine receptors. *J Neurosci* **11:**837–845.
Lowry OH, Rosebrough NH, Farr AC and Randall RT (1951) Protein measurement with the Folin phenol reagent. *J Biol Chem* **193:**265–275.
Lukas RJ (1989) Pharmacological distinctions between functional nicotinic acetylcholine receptors on PC12 rat pheochromocytoma and TE671 human medulloblastoma. *J Pharmacol Exp Ther* **251:**175–182.
Marks MJ, Bullock AE and Collins AC (1995) Sodium channels blockers partially inhibit nicotine-stimulated $^{86}Rb^+$ efflux from mouse brain synaptosomes. *J Pharmacol Exp Ther* **274:**833–841.
Marks MJ, Farnham DA, Grady SR and Collins AC (1993) Nicotinic receptor function determined by stimulation of rubidium efflux from mouse brain synaptosomes. *J Pharmacol Exp Ther* **264:**542–552.
Marks MJ, Pauly JR, Gross SD, Deneris ED, Hermans-Borgmeyer I, Heinemann SF and Collins AC (1992) Nicotine binding and nicotinic receptor subunit RNA after chronic nicotine treatment. *J Neurosci* **12:**2765–2784.
Marks MJ, Robinson SF and Collins AC (1996) Nicotinic agonists differ in activation and desensitization of $^{86}Rb^+$ efflux from mouse thalamic synaptosomes. *J Pharmacol Exp Ther* **277:**1383–1396.
Marks MJ, Smith KW and Collins AC (1998) Differential agonist inhibition identifies multiple epibatine binding sites in mouse brain. *J Pharmacol Exp Ther* **285:**377–386.
Marks MJ, Stitzel JA, Romm E, Wehner JM and Collins AC (1986) Nicotinic binding sites in rat and mouse brain: Comparison of acetylcholine, nicotine and α-bungarotoxin. *Mol Pharmacol* **30:**427–436.
Mulle C, Vidal C, Benoit P and Changeux J-P (1991) Existence of different subtypes of nicotinic acetylcholine receptors in the rat habenulo-interpeduncular system. *J Neurosci* **11:**2588–2597.
Picciotto MR, Zoli M, Lena C, Bessis A, Lallemand Y, LeNovere N, Vincent P, Merlo Pich E, Brulet P and Changeux J-P (1995) Abnormal avoidance learning in mice lacking functional high-affinity nicotine receptor in brain. *Nature (Lond)* **374:**65–67.
Ramirez-Latorre J, Yu CR, Qu X, Perin F, Karlin A and Role L (1996) Functional contributions of α5 subunit to neuronal acetylcholine receptor channels. *Nature (Lond)* **380:**347–351.
Sacaan AI, Dunlop JL and Lloyd GK (1995) Pharmacological characterization of neuronal acetylcholine gated ion channel receptor-mediated hippocampal norepinephrine and striatal dopamine release from rat brain slices. *J Pharmacol Exp Ther* **274:**224–230.
Sargent PB (1993) The diversity of neuronal nicotinic acetylcholine receptors. *Annu Rev Neurosci* **16:**403–443.
Seguela P, Wadiche J, Dinely-Miller K, Dani J and Patrick J (1993) Molecular cloning, functional properties, and distribution of rat brain α7: A nicotinic channel highly permeable to calcium. *J Neurosci* **13:**596–604.
Sullivan JP, Donnelly-Roberts D, Briggs CA, Anderson DJ, Gopalakrishnan M, Piattoni-Kaplan M, Campbell JE, McKenna DG, Molinari E, Hettinger AM, Garvey DS, Wasicak JT, Holladay MW, Williams M and Arneric SP (1996) A-85380 [3-(2-(S)-azetidinylmethoxypyridine]: In vitro pharmacological properties of a novel, high affinity alpha4 beta2 nicotinic acetylcholine receptor ligand. *Neuropharmacology* **35:**725–734.
Wada E, McKinnon D, Heinemann S, Patrick J and Swanson LW (1990) The distribution of MRNA encoded by a new member of the neuronal nicotinic acetylcholine receptor gene family (α5) in the rat central nervous system. *Brain Res* **526:**45–53.
Wada E, Wada K, Boulter J, Deneris E, Heinemann S, Patrick J and Swanson LW (1989) Distribution of alpha-2, alpha-3, alpha-4 and beta-2 neuronal nicotinic receptor subunit mRNAs in the central nervous system: A hybridization histochemical study in the rat. *J Comp Neurol* **284:**314–335.
Wang F, Gerzanich V, Wells GB, Anand R, Peng X, Keyser K and Lindstrom J (1996) Assembly of human neuronal nicotinic receptor alpha5 subunits with alpha3, beta2 and beta4 subunits. *J Biol Chem* **271:**17656–17665.
Whiting PJ and Lindstrom J (1988) Characterization of bovine and human neuronal nicotinic acetylcholine receptors using monoclonal antibodies. *J Neurosci* **8:**3395–3404.
Wonnacott S (1997) Presynaptic nicotinic Ach receptors. *Trends Neurosci* **20:**92–98.
Yu ZJ, Morgan DG and Wecker L (1996) Distribution of three nicotinic receptor α4 mRNA transcripts in rat brain: Selective regulation by nicotine administration. *J Neurochem* **66:**1326–1329.
Zoli M, Lena C, Picciotto MR and Changeux J-P (1998) Identification of four classes of nicotinic receptors using beta2 mutant mice. *J Neurosci* **18:**4461–4472.

Send reprint requests to: Dr. Allan C. Collins, Ph.D., Institute for Behavioral Genetics, Campus Box 447, University of Colorado, Boulder, CO 80309. E-mail: al.collins@colorado.edu